BJP British Journal of Pharmacology

DOI:10.1111/j.1476-5381.2011.01715.x
www.brjpharmacol.org

RESEARCH PAPER

Transient receptor potential melastatin 4 inhibitor 9-phenanthrol abolishes arrhythmias induced by hypoxia and re-oxygenation in mouse ventricle

Christophe Simard, Laurent Sallé, René Rouet and Romain Guinamard

Groupe Cœur et Ischémie, Université de Caen, Caen, France

Correspondence
Romain Guinamard, Groupe Cœur et Ischémie, EA3212, Université de Caen, Sciences D, 14032 Caen Cedex, France.
E-mail: romain.guinamard@unicaen.fr

Keywords
arrhythmias; action potential; early afterdepolarization; TRP; TRPM4; 9-phenanthrol; flufenamic acid; hypoxia; re-oxygenation

Received
22 April 2011
Revised
21 September 2011
Accepted
23 September 2011

BACKGROUND AND PURPOSE

Hypoxia and subsequent re-oxygenation are associated with cardiac arrhythmias such as early afterdepolarizations (EADs), which may be partly explained by perturbations in cytosolic calcium concentration. Transient receptor potential melastatin 4 (TRPM4), a calcium-activated non-selective cation channel, is functionally expressed in the heart. Based on its biophysical properties, it is likely to participate in EADs. Hence, modulators of TRPM4 activity may influence arrhythmias. The aim of this study was to investigate the possible anti-arrhythmic effect of 9-phenanthrol, a TRPM4 inhibitor in a murine heart model of hypoxia and re-oxygenation-induced EADs.

EXPERIMENTAL APPROACH

Mouse heart was removed, and the right ventricle was pinned in a superfusion chamber. After a period of normoxia, the preparation was superfused for 2 h with a hypoxic solution and then re-oxygenated. Spontaneous electrical activity was investigated by intracellular microelectrode recordings.

KEY RESULTS

In normoxic conditions, the ventricle exhibited spontaneous action potentials. Application of the hypoxia and re-oxygenation protocol unmasked hypoxia-induced EADs, the occurrence of which increased under re-oxygenation. The frequency of these EADs was reduced by superfusion with either flufenamic acid, a blocker of Ca^{2+}-dependent cation channels or with 9-phenanthrol. Superfusion with 9-phenanthrol (10^{-5} or 10^{-4} mol·L^{-1}) caused a dramatic dose-dependent abolition of EADs.

CONCLUSIONS AND IMPLICATIONS

Hypoxia and re-oxygenation-induced EADs can be generated in the mouse heart model. 9-Phenanthrol abolished EADs, which strongly suggests the involvement of TRPM4 in the generation of EAD. This identifies non-selective cation channels inhibitors as new pharmacological candidates in the treatment of arrhythmias.

Abbreviations

AP, action potential; APD, action potential duration; CFTR, cystic fibrosis transmembrane conductance regulator; EADs, early afterdepolarizations; H-89, *N*-[2-(*p*-bromocinnamylamino)ethyl]-5-isoquinolinesulphonamidedihydrochloride hydrate; $I_{Ca,L}$, L-type calcium current; I_K, potassium current; RMP, resting membrane potential; TRP, transient receptor potential; TRPM4, transient receptor potential melastatin 4

Introduction

Myocardial ischaemia is associated with drastic changes in ATP levels, which result mainly from hypoxia, leading to disturbances in the ionic concentrations such as accumulation of $[K^+]_o$, $[Na^+]_i$, $[Ca^{2+}]_i$ (Carmeliet, 1999). Among these, $[Ca^{2+}]_i$ plays a crucial role because of the sensitivity of many processes to this ion. Diastolic $[Ca^{2+}]_i$ increases within a few minutes in mammalian heart models of ischaemia or hypoxia (Kihara *et al.*, 1989; Siegmund *et al.*, 1992). Upon reperfusion, the kinetics of $[Ca^{2+}]_i$ variations depend on the model, but it usually results in a secondary increase in $[Ca^{2+}]_i$ associated with oscillations (Carmeliet, 1999). This $[Ca^{2+}]_i$ overload is in part responsible for the occurrence of triggered activities arising before the end of the action potential (AP) repolarization, called early afterdepolarizations (EADs), leading to arrhythmias. Indeed, while EADs that occur during the plateau phase of the AP are due to re-activation of Ca^{2+} channels, those that occur late in repolarization, are attributable to Ca^{2+}-activated currents (Priori *et al.*, 1990; Benndorf *et al.*, 1991a; Bers, 2001).

$[Ca^{2+}]_i$-sensitive effectors that are capable of slowing down the repolarization and thus prolonging the action potential are key players in EAD induction (Carmeliet, 1999). Among these, transient receptor potential melastatin 4 (TRPM4) is a new candidate, the contribution of which was suggested previously (Guinamard *et al.*, 2006). TRPM4 is a non-selective cation channel cloned in 2002 (Launay *et al.*, 2002) that is almost ubiquitously expressed in tissues and the physiological roles of this channel are now emerging (Guinamard *et al.*, 2010). According to biochemical data, the heart shows one of the highest levels of expression of TRPM4 (Launay *et al.*, 2002). Moreover, its functional expression was demonstrated by electrophysiological investigations in mouse sino-atrial node (Demion *et al.*, 2007), human atrium (Guinamard *et al.*, 2004) and spontaneously hypertensive rat ventricle (Guinamard *et al.*, 2006). The relative expression of TRPM4 transcripts, assayed by quantitative RT-PCR in non-diseased human hearts indicated that the channel is expressed more in Purkinje fibres than in septum, atrium and ventricles (Kruse *et al.*, 2009). In addition, two recent studies reported mutations in the human TRPM4 associated with cardiac conduction block (Kruse *et al.*, 2009; Liu *et al.*, 2010). Despite these reports, the physiological and pathological role of TRPM4 in heart function remains poorly understood. By producing cell depolarization during calcium overload, TRPM4 probably participates in cardiac perturbations such as afterdepolarizations observed during the reperfusion after ischaemia.

In a recent study, we demonstrated that TRPM4, expressed heterologously in HEK-293 cells, is inhibited by 9-phenanthrol, a benzo[c]quinolizinium derivative (Grand *et al.*, 2008). 9-Phenanthrol was very recently shown to be suitable for physiological studies. Indeed, it has been used to modulate cerebral arterial constriction, in which it acts through inhibition of pressure-induced smooth muscle depolarization, when applied at 10^{-4} mol·L^{-1} (Gonzales *et al.*, 2010a,b). In addition, 9-phenanthrol eliminates *N*-methyl D-aspartate-induced burst firing in nigrostriatal dopaminergic neurons, when applied at 10^{-4} mol·L^{-1} (Mrejeru *et al.*, 2011). Interestingly, flufenamic acid, another TRPM4 blocker, reproduces these effects (Gonzales *et al.*, 2010a; Mrejeru *et al.*, 2011). According to these results on excitable cells, we hypothesized that 9-phenanthrol and flufenamic acid would be able to modulate hypoxia and reperfusion-induced cardiac arrhythmias.

The aim of the present study was to investigate the effect of 9-phenanthrol on cardiac arrhythmias. A mouse heart model was developed to induce arrhythmia in conditions of hypoxia followed by re-oxygenation. Action potentials were recorded in the mouse ventricles using a standard intracellular microelectrode technique. Superfusion with 9-phenanthrol led to a dose-dependent decrease in the occurrence of EADs. This is the first report of an anti-arrhythmic action of 9-phenanthrol.

Methods

Heart sampling

All animal care and experimental procedures complied with the Guidelines of the European Commission Directive 86/609/EEC and were approved by the local Ethics Committee. Adult female C57/BL6JRj mice (4–6 weeks) were killed by cervical dislocation, and the heart was quickly removed. The left ventricle was ablated, while the right ventricle was opened and pinned down, with the endocardial surface upwards, in a superfusion chamber. When specified, pieces of the right ventricle free wall were isolated and similarly placed in the chamber. The chamber was superfused at the rate of 7 mL min^{-1} with a physiological solution bubbled with 95% O_2 and 5% CO_2 and maintained at 37°C. The composition of the standard physiological solution (pH 7.4) was (in mmol·L^{-1}): NaCl 108.2, KCl 4, $CaCl_2$ 1.8, $MgCl_2$ 1.0, NaH_2PO_4 1.8, $NaHCO_3$ 25, glucose 11. When specified, the solution was buffered with HEPES, using the following composition (in mmol·L^{-1}): NaCl 140, KCl 5.4, $CaCl_2$ 1.8, $MgCl_2$ 2.1, NaH_2PO_4 0.3, HEPES 10, glucose 11.

Experimental protocol

The right ventricle fragment was superfused in standard, normoxic conditions (physiological solution saturated with 95% O_2 and 5% CO_2) for 15 min. It was then exposed to hypoxic conditions by turning off the bubbling of the physiological solution for 2 h. At the end of the hypoxic episode, the ventricle was superfused with the initial oxygenated solution, simulating re-oxygenation. Drugs were added for 10 min in the superfusion solution either during the hypoxic or re-oxygenation episode, as specified in the text.

Flufenamic acid and 9-phenanthrol were dissolved in dimethylsulphoxide (DMSO) to a maximum final DMSO concentration of 0.1% that had no effect on ventricular action potential (data not shown). The control solution had the same concentration of DMSO.

N-[2-(*p*-bromocinnamylamino)ethyl]-5-isoquinolinesulphonamidedihydrochloride hydrate (H-89) was dissolved in water.

Drug/molecular target nomenclature conforms to BJP's *Guide to Receptors and Channels* (Alexander *et al.*, 2011).

Action potential acquisition and analysis

Transmembrane potentials were recorded by conventional intracellular microelectrode technique, using a glass micro-

electrode filled with KCl (3 mol·L^{-1}) with tip resistance around 10 MΩ. The microelectrodes were coupled to the input stages of an in-house impedance capacitance-neutralizing amplifier. The recordings were displayed and analysed using a cardiac action potential (AP) automatic acquisition software (iox 2, Emka Technologie, France) providing AP rate, resting membrane potential (RMP), action potential duration at 50% (APD_{50}), 70% (APD_{70}) and 90% (APD_{90}) of repolarization. No electrical stimulation was applied, allowing recording of the free activity of the ventricle. The number of EAD was determined by visual screening of the recordings. An event was considered as an EAD when additional depolarization occurred during AP repolarization, before completion of total repolarization (see representative traces in Figure 1A). To evaluate the variation of EAD frequency, the number of EAD per 10 s were recorded and normalized to the number of AP in the same period (EAD/AP).

Partial oxygen pressure (pO_2) in the physiological solution was measured using a Z900 electrode oxymeter (Consort, Turnhout, Belgium). The solution was saturated by bubbling for one hour with 95% O_2, 5% CO_2. Bubbling was thus turned off, and pO_2 was measured during the two hours of hypoxia. For re-oxygenation, the hypoxic solution was changed suddenly to the saturated solution.

Isolation of mouse ventricular myocytes

Myocytes were isolated from mice ventricles using an adapted enzymatic dissociation protocol (Sallé *et al.*, 2008). Briefly, after the mice had been killed, the heart was rapidly removed and mounted on a Langendorff apparatus and perfused retrogradely with a HEPES-based isolation solution containing (in mmol·L^{-1}): NaCl 130, KCl 5.4, NaH_2PO_4 0.4, $MgCl_2$ 1.4, $CaCl_2$ 1, HEPES 10, glucose 10, taurine 20 and creatine 10 (pH 7.4 with NaOH). When the coronary circulation had been cleared of blood, perfusion was continued with Ca-free isolation solution (in which $CaCl_2$ was replaced with 0.1 mmol·L^{-1} EGTA) for 4 min, followed by perfusion for a further 15–17 min with isolation solution containing 0.3 mg·mL^{-1} collagenase (type I; Worthington Biochemical, Lakewood, NJ, USA), and 0.08 mg·mL^{-1} protease (type XIV; Sigma, L'Isle d'Abeau Chesnes, France) supplemented with 1% BSA. The ventricles were then excised from the heart, minced, and gently shaken at 37°C in enzyme-containing solution. Ventricular cells were filtered from this solution and resuspended in isolation solution containing 1 mmol·L^{-1} Ca^{2+}. All experiments were performed at room temperature (20–23°C).

Calcium and potassium current recordings

Myocytes were studied in Petri dishes on the stage of an inverted microscope (Nikon TE2000, Tokyo, Japan). Currents were recorded using the whole-cell configuration of the patch clamp technique. An Axopatch 200B (Axon Instruments, Sunnyvale, CA, USA) amplifier was used, controlled by a Pentium PC connected via a Digidata 1322A A/D converter (Axon Instruments), which was also used for data acquisition and analysis using pClamp software (Axon Instruments). Signals were filtered at 2 kHz using an eight-pole Bessel low-pass filter before digitization at 10 kHz and storage. Patch pipettes resistance was typically 0.8–1.2 MΩ when filled with intracellular solution (below).

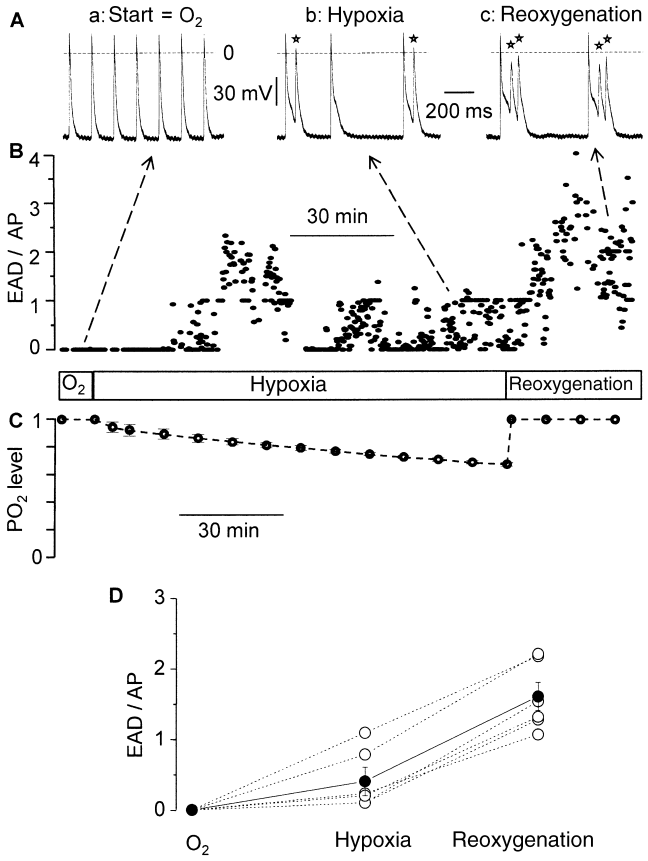

Figure 1

Hypoxia–re-oxygenation-induced arrhythmias. (A) Action potentials were recorded in a mouse ventricle superfused with a standard, oxygenated solution (a), followed by a hypoxic solution (b), followed by the oxygenated solution again (c). EADs are indicated by stars. Bars represent time interval (ms) or voltage (mV) as indicated. (B) The number of EADs recorded as above were normalized to that of action potentials (EAD/AP) for 10 s periods and plotted against time. Same experiment as in (A). Arrows indicate the time corresponding to a, b and c recordings. Bar represents a 30 min interval. (C) pO_2 in the superfused solution, normalized to the value of a saturated solution, recorded during the above hypoxia–re-oxygenation protocol (mean ± SEM; $n = 4$). (D) Number of EAD/AP is compared for the three phases: start (O_2), hypoxia and re-oxygenation. Open circles linked by dotted lines indicate single experiments, while black circles linked by black line correspond to the mean of experiments (mean ± SEM; $n = 6$).

L-type calcium current ($I_{Ca,L}$) was measured using Na^+- and K^+-free external and internal solutions to avoid contamination by overlapping ionic currents (Brette *et al.*, 2006). The external solution contained (in mmol·L^{-1}): 4AP 5, TEACl 130, $MgCl_2$ 0.5, HEPES 10, Glucose 10, $CaCl_2$ 1, pH set to 7.4 using TEAOH. The pipette solution contained (in mmol·L^{-1}) CsCl 110, TEACl 20, $MgCl_2$ 0.5, Mg-ATP 5, EGTA 5, HEPES 10, GTP–Tris 0.4, set to pH 7.2 with CsOH. $I_{Ca,L}$ was elicited by a 300 ms rectangular step to 0 mV (from a holding potential of –80 mV) at 0.1 Hz and measured as the difference between the peak current and current at the end of the pulse.

K^+ currents were recorded with the HEPES-based salt solution (above) but with 1 mmol·L^{-1} $CdCl_2$ to block Na^+–Ca^{2+}

exchange, fast Na^+ and Ca^{2+} currents. The pipette solution contained (in mmol·L^{-1}) KCl 140, $MgCl_2$ 0.5, Mg-ATP 5, EGTA 5, HEPES 10, GTP–Tris 0.4 set to pH 7.3 with KOH. To evoke potassium currents, a 150 ms test step to +30 mV (i.e. approximate peak of action potential overshoot) from a holding potential of –80 mV was applied for 150 ms. A 50 ms prepulse to –40 mV was used to ensure full inactivation of fast Na^+ current during the test pulse. With this protocol, it was possible to record at least four components of K current in mice ventricular myocytes (see Nerbonne and Kass, 2005). Thus, the area (integral) between the current trace activated by the depolarizing pulse and the zero current level representing global charge carrying by K^+ at +30 mV was analysed. Experimental conditions described above exclude contribution of other ions to the outward current. Cells showing a variation in I_{hold} (i.e. current at –80 mV) during experiments likely to alter our area measurements at +30 mV were discarded.

Data analysis

Results are reported as mean ± SEM. To compare occurrence of EAD/AP in different experimental conditions, data were tested for normality by a Shapiro–Wilk test (normality accepted for $P > 0.05$), then compared using Student's paired *t*-test. Student's unpaired *t*-test was used when comparing data from a different batch of experiments. Statistical analysis was performed using Sigma Plot software v.11 (Systat, Chicago, IL, USA). Values of $P < 0.05$ were taken to indicate statistically significant differences; *n* refers to the number of experiments conducted and the number of mice used.

Results

Spontaneous activity in right ventricle

The first set of experiments was designed to characterize the free ventricular electrical activity from the whole right ventricle. In the initial superfusion with standard oxygenated solution, ventricles exhibited an initial spontaneous AP activity (Figure 1A, left). The mean beating rate was 384.4 ± 11.9 beats min^{-1} ($n = 10$ mice) in oxygenated conditions. RMP was –74.4 ± 1.2 mV and action potential durations for 50%, 70% and 90% of repolarization (APD_{50}, APD_{70} and APD_{90}) were 10.2 ± 0.6, 17.3 ± 1.1, 37.3 ± 2.4 ms ($n = 10$), respectively, which is agreement with previous reports on such preparations (Anumonwo *et al.*, 2001). No EADs were observed in these initial oxygenated conditions ($n = 10$ mice).

To identify the origin of this spontaneous activity, we evaluated the activity from isolated free wall pieces of the right ventricle that contain less conductive tissue than the septum. Only 3 out of the 11 specimens exhibited spontaneous activity, while others did not. Moreover, the beating rate of the three active specimens was 236 ± 7.6 beats min^{-1}, which is significantly smaller than whole right ventricle preparations (unpaired *t*-test, $P < 0.00005$). This suggests that the free activity is correlated with the abundance of conductive tissue.

Hypoxia–re-oxygenation-induced arrhythmias

Hypoxia and re-oxygenation were induced in whole right ventricle preparations. After 15 min in normoxia, the preparation was superfused for 2 h with the standard physiological solution without oxygenation. The pO_2 measured in the superfused solution decreased progressively with time and was significantly reduced by 33.0 ± 1.2% ($n = 4$, paired *t*-test, $P < 0.0005$) after 2 h (Figure 1C). EAD appeared in all experiments ($n = 6$) starting at 14.7 ± 3.4 min of hypoxic conditions when the pO_2 was reduced by only 10% (Figure 1A,B). At the end of the 2 h of hypoxia, EADs were detected with a frequency of 0.4 ± 0.2 EAD/AP ($n = 6$). After 2 h of hypoxic conditions, the superfusion was switched back to the oxygenated solution, restoring the initial pO_2 level. This step is referred to as re-oxygenation conditions in the following text. EAD frequency was significantly enhanced to 1.6 ± 0.2 EAD/AP in re-oxygenation conditions ($n = 6$, paired *t*-test, $P < 0.0001$ when compared with hypoxia) (Figure 1D).

We disregarded APD and beat rate variations under hypoxia and re-oxygenation from further study because the presence of EADs strongly modifies these parameters rendering their significance questionable.

To ensure that EADs were induced by hypoxia and re-oxygenation, five recordings were performed for 2.5 h with permanent superfusion of oxygenated solution. EADs were detected only episodically with an occurrence increasing with time of superfusion to reach the low level of 0.1 ± 0.1 EAD/AP ($n = 5$) at the end of the 2.5 h. This occurrence is significantly smaller than those observed after hypoxia and re-oxygenation (unpaired *t*-test, $P < 0.05$). Note that in these control experiments, no significant variation of beating rate was observed during the 2.5 h with superfusion of oxygenated solution.

In our model where pH is equilibrated with $NaHCO_3$, pH variations may occur when CO_2 bubbling is interrupted and may thereby impact EADs. Hence, the effects of hypoxia and re-oxygenation on EADs under conditions in which pH was buffered with HEPES were investigated. Under these conditions, the hypoxia and re-oxygenation protocol was similarly able to induce EADs [0.7 ± 0.4 EAD/AP ($n = 6$) in hypoxia and 1.2 ± 0.6 EAD/AP ($n = 6$) in re-oxygenation]. This indicates that the EADs recorded in our model are not induced by changes in external pH.

Anti-arrhythmic effect of 9-phenanthrol

We used the protocol of hypoxia and re-oxygenation described in the previous section to induce EADs and evaluate whether the TRPM4 inhibitor 9-phenanthrol is able to modulate their occurrence.

9-Phenanthrol at 10^{-5} or 10^{-4} mol·L^{-1} was added to the oxygenated solution within the re-oxygenation episode (see grey box in Figure 2B) and reduced the number of EADs occurring (Figure 2). 9-Phenanthrol at 10^{-5} mol·L^{-1} applied for 10 min significantly reduced the number of EAD by 59.5 ± 12.3% (1.8 ± 1.4 EAD/AP compared with 2.8 ± 1.7 EAD/AP in control, paired *t*-test, $P < 0.05$, $n = 6$). Moreover, 9-phenanthrol at 10^{-4} mol·L^{-1} totally suppressed EADs in all experiments after 3.1 ± 0.7 min of superfusion ($n = 6$) (Figure 2A). A representative experiment depicted in Figure 2B shows the time course of 9-phenanthrol effect. The effect of 9-phenanthrol was partly reversed by washing (oxygenated physiological solution) in all experiments.

We measured the effect of 9-phenanthrol on the resting membrane potential (RMP) in re-oxygenation conditions.

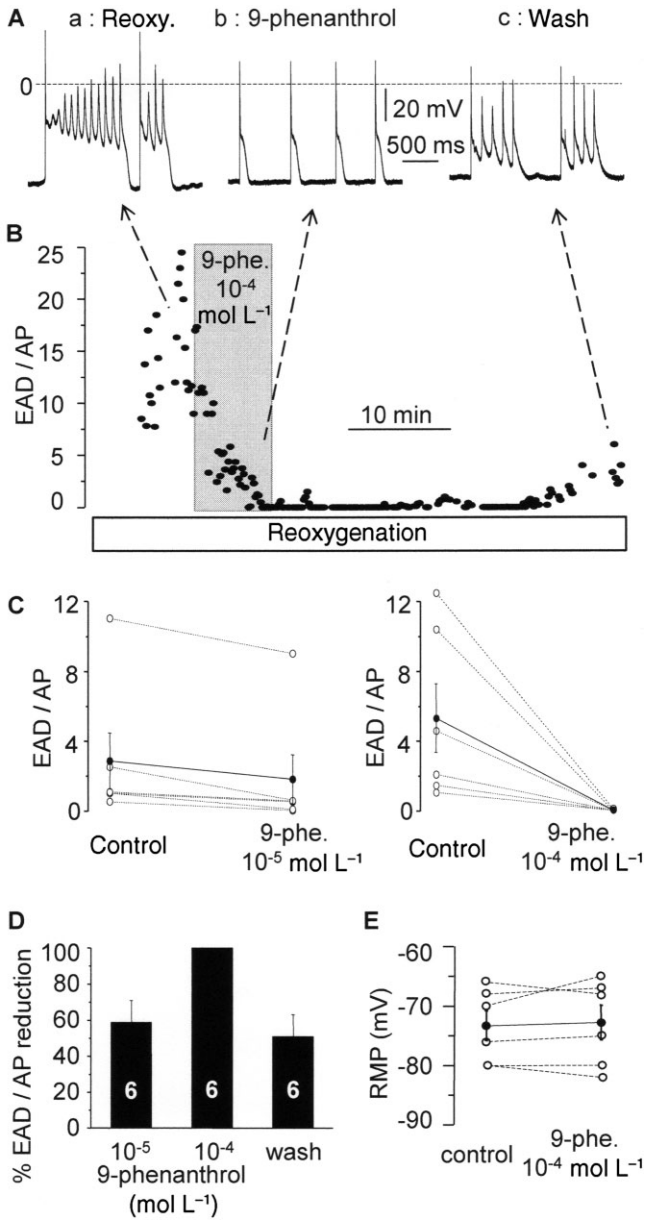

Figure 2

Anti-arrhythmic effect of 9-phenanthrol. (A) Action potentials recorded in a mouse ventricle during re-oxygenation in the standard solution (a), or in the presence of 9-phenanthrol, 10^{-4} mol·L^{-1} (b), or after washout of 9-phenanthrol (c). Bars represent time interval (ms) or voltage (mV) as indicated. (B) Number of EAD/AP for 10 s periods during re-oxygenation for the above a, b and c phases, as indicated. The phase of superfusion with 9-phenanthrol, 10^{-4} mol·L^{-1}, is highlighted in grey. Bar represents a 10 min interval. (C) Number of EAD/AP after re-oxygenation before and during superfusion of 10^{-5} or 10^{-4} mol·L^{-1} 9-phenanthrol. Open circles linked by dotted lines indicate single experiments while black circles linked by black line correspond to the mean of experiments (mean ± SEM; n = 6). (D) Reduction in EAD/AP (mean ± SEM) during superfusion with 10^{-5} or 10^{-4} mol·L^{-1} 9-phenanthrol, followed by washing with standard solution, given as a percentage of the value during re-oxygenation before application of the drug and calculated as follows: % reduction = 100 − [(EAD/AP with inhibitor)/(EAD/AP in control) x 100]. (E) Resting membrane potential variation induced by 9-phenanthrol 10^{-4} mol·L^{-1}. Open circles linked by dotted lines indicate single experiments while black circles linked by black line correspond to the mean of the 6 experiments. Control corresponds to RMP in re-oxygenation solution before application of the drug.

The RMP was not affected by 9-phenanthrol even at 10^{-4} mol·L^{-1} (non-significant variations of 0.3 ± 0.4 mV for 10^{-5} mol·L^{-1}, n = 6 and +0.5 ± 2.5 mV for 10^{-4} mol·L^{-1}, paired t-test, NS, n = 6) (Figure 2E).

The anti-arrhythmic effect of 9-phenanthrol was not restricted to re-oxygenation-induced arrhythmias since it also reduced the occurrence of hypoxia-induced EADs. Indeed, 9-phenanthrol at 10^{-5} mol·L^{-1} applied for 10 min during the hypoxic episode reduced the number of EADs occurring by 76.4 ± 11% (n = 5), while 9-phenanthrol at 10^{-4} mol·L^{-1} totally suppressed EADs in all experiments (n = 3). Once again, no significant variation in RMP was detected after application of 9-phenanthrol.

Effect of 9-phenanthrol on $I_{Ca,L}$ and I_K

Because $I_{Ca,L}$ is one of the major currents responsible for EADs, we investigated the effect of 9-phenanthrol on this current recorded on freshly isolated mouse ventricular myocytes, using the whole-cell configuration of the patch-clamp technique. Application of 9-phenanthrol at 10^{-5} mol·L^{-1} had no effect on $I_{Ca,L}$ density (3.1 ± 0.8 pA/pF vs. 3.2 ± 0.7 pA/pF in control and 9-phenanthrol 10^{-5} mol·L^{-1}, respectively, paired t-test, NS, n = 6) but 9-phenanthrol at 10^{-4} mol·L^{-1} reversibly reduced the current density by 47% (3.4 ± 0.5 pA/pF vs. 1.8 ± 0.5 pA/pF in control and 9-phenanthrol 10^{-4} mol·L^{-1}, respectively, paired t-test, $P < 0.05$, n = 6) (Figure 3A,B).

Activation of potassium channels may reduce EADs induction by accelerating cell repolarization. We thus investigated the effect of 9-phenanthrol on I_K in ventricular myocytes. Application of 9-phenanthrol at 10^{-5} mol·L^{-1} had no effect on the whole K current estimated by the charge carried by K (3.3 ± 0.6 pC/pF vs. 3.0 ± 0.5 pC/pF in control and 9-phenanthrol 10^{-5} mol·L^{-1} treated preparations, respectively, paired t-test, NS, n = 5), whereas 9-phenanthrol at 10^{-4} mol·L^{-1} reversibly reduced K current by 43% (3.0 ± 0.3 pC/pF vs. 1.7 ± 0.1 pC/pF in control and 9-phenanthrol 10^{-4} mol·L^{-1}, respectively, paired t-test, $P < 0.05$, n = 5) (Figure 3C,D).

Lack of PKA contribution

A previous study has suggested a possible inhibition of bovine cAMP-dependent protein kinase catalytic subunit (PKA) by phenanthrene derivatives (Wang *et al.*, 1994). We investigated whether this action might be involved in the anti-arrhythmic effect of 9-phenanthrol. After induction of arrhythmias by the hypoxia–reoxygenation protocol, the PKA inhibitor H-89 at 10^{-6} mol·L^{-1} was added during re-oxygenation (referred to as control conditions). At this concentration, the isoquinoline derivative H-89 is known to be specific for PKA (Chijiwa *et al.*, 1990; Lochner and Moolman, 2006) and has an inhibitory effect on PKA-mediated parameters on isolated heart (Robinet *et al.*, 2005). H-89 applied for 10 min did not significantly affect arrhythmias (1.1 ± 0.4 EAD/AP compared with 1.0 ± 0.4 EAD/AP in

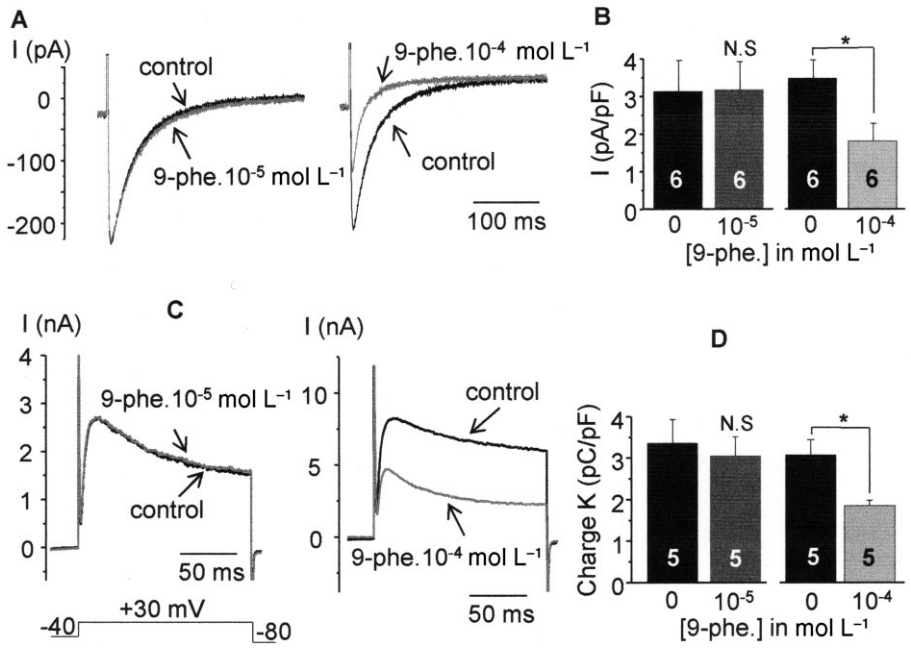

Figure 3

9-Phenanthrol effect on $I_{Ca,L}$ and I_K. (A) Representative example of 9-phenanthrol effect (10^{-5} mol·L^{-1}, left, and 10^{-4} mol·L^{-1}, right) on L-type calcium current elicited by a 300 ms step from –80 to 0 mV in mouse ventricular myocytes. (B) Means ± SEM of 9-phenanthrol effect on L-type calcium current (in pA/pF). Number of cells is indicated in each column. (NS: not significant, * indicates $P < 0.05$). (C) Representative example of 9-phenanthrol effect (10^{-5} mol L^{-1}, left, and 10^{-4} mol L^{-1}, right) on K current elicited by voltage step (bottom) in mouse ventricular myocytes. (D) Means ± SEM of 9-phenanthrol effect (10^{-5} mol L^{-1} left and 10^{-4} mol L^{-1} right) on global charge carrying by potassium (in pC/pF).

control, paired *t*-test, NS, $n = 3$) (Figure 4). The resting membrane potential was –70 ± 1 mV in control, compared with –69.7 ± 0.9 mV in the presence of H-89, corresponding to a non-significant variation of –0.3 ± 1.2 mV (paired *t*-test, NS, $n = 3$). The superfusion of 9-phenanthrol at 10^{-4} mol·L^{-1} in the presence of 10^{-6} mol·L^{-1} H-89 totally suppressed arrhythmias in the three experiments performed (Figure 4). No significant effect on resting membrane potential was induced by 9-phenanthrol in the presence of H-89 (variation of –1.2 ± 0.8 mV, paired *t*-test, NS, $n = 3$). In view of these results, the anti-arrhythmic effect of 9-phenanthrol appears to be independent of PKA.

Effect of flufenamic acid

We investigated the effect of the less selective but most commonly used TRPM4 inhibitor flufenamic acid on hypoxia–reoxygenation-induced EADs. The latter was superfused at a concentration of 10^{-5} mol·L^{-1}, which has been shown to inhibit 70% of TRPM4 currents in the HEK-293 cells as well as in native cardiomyocytes (Ullrich *et al.*, 2005; Guinamard *et al.*, 2006). Higher concentrations were not used in order to minimize effects on other targets (see Discussion). Flufenamic acid (10^{-5} mol·L^{-1}) significantly reduced the hypoxia–reoxygenation-induced arrhythmias (0.3 ± 0.2 compared with 1.9 ± 0.4 EAD/AP in control, paired *t*-test, $P < 0.0001$, $n = 5$) (Figure 5). This effect was reversible as shown in Figure 4. Interestingly, EAD re-appeared within a minute after washing of flufenamic acid, while recovery was delayed after 9-phenanthrol superfusion (compare Figures 2B and 5B). Additionally, no significant variation in RMP was induced by flufenamic acid superfusion (variation of –0.5 ± 0.3 mV, paired *t*-test, NS, $n = 5$).

Discussion

Hypoxia and re-oxygenation protocol

The first intriguing observation in our study was the permanent and regular free beating activity of the ventricles. According to the fact that, in our preparation, atria was removed, the pacemaker activity did not come from sinus node but most likely from the atrioventricular node or conductive tissue. Indeed, the spontaneous activity is lower in pieces isolated from the free wall compared with specimens in which the entire right ventricle is preserved. Such spontaneous activity originating from conductive tissue has been reported in mouse isolated right ventricle, albeit without detailed analysis (Anumonwo *et al.*, 2001). The present study did not evaluate the effect of drugs on this activity but focused only on the occurrence of EADs referred to as arrhythmias. As shown by the results, EADs are very rare and episodic in oxygenated conditions.

The protocol for simulating hypoxia and re-oxygenation described here successfully induced reproducible and frequent arrhythmias. Other protocols for induction of EADs in mouse ventricle either by long cycle length stimulation or by application of caesium to block K^+ channels have been reported to be difficult to implement and not sufficiently

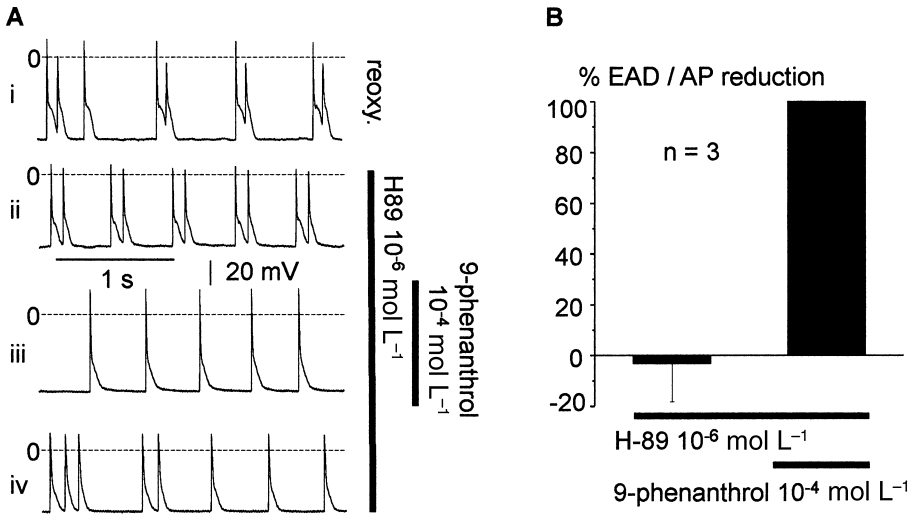

Figure 4

Anti-arrhythmic effect of 9-phenanthrol is independent of PKA. (A) Action potential recordings in a mouse ventricle under re-oxygenation in four successive superfusion solutions: (i) initial re-oxygenation without drug, (ii) re-oxygenation with solution containing H-89 10^{-6} mol·L^{-1}, (iii) re-oxygenation with solution containing H-89, 10^{-6} mol·L^{-1} + 9-phenanthrol, 10^{-4} mol·L^{-1} or (iv) re-oxygenation with solution containing H-89, 10^{-6} mol·L^{-1} with washout of 9-phenanthrol. Bars represent time interval (ms) or voltage (mV) as indicated. Note that superfusion with H-89 does not suppress EADs, while that with 9-phenanthrol does. (B) Percentage reduction of EAD/AP (mean ± SEM) due to superfusion with re-oxygenation solution containing H-89 (10^{-6} mol·L^{-1}) alone or H-89 (10^{-6} mol·L^{-1}) + 9-phenanthrol (10^{-4} mol·L^{-1}) (n = 3) compared with initial re-oxygenation solution without the drugs.

reproducible (Shen and Liu, 1993; Zhou and Liu, 1997). Interestingly, a mouse Langendorff model of ischaemia-induced ventricular fibrillation was recently described in which arrhythmias occurred in ischaemia and were exacerbated in reperfusion (Stables and Curtis, 2009). In this model, an increased number of arrhythmias occurred within minutes after re-oxygenation, similar to our results but different from other species in which they occurred within seconds (Stables and Curtis, 2009). As stated by Stables and Curtis (2009), because the time profile of re-oxygenation-induced arrhythmias is not known in humans, these characteristics in the mouse do not exclude it as a clinically relevant model.

Our model simulates hypoxia and re-oxygenation, but not necessarily the consequences of ischaemia and reperfusion observed *in vivo*. Indeed, ischaemia results not only in hypoxia but also in metabolic and neurohormonal perturbations that play a critical role during *in vivo* reperfusion. The hypoxic level obtained in our model (pO_2 reduction by 33% after 2 h of hypoxia) is about half the level obtained by a complete replacement of O_2 with N_2 bubbling (reduction of 65%) (Sugimoto *et al.*, 1995). Hence, it is possible that moderate hypoxia is sufficient to induce EADs.

Anti-arrhythmic effect of 9-phenanthrol and possible targets

An anti-arrhythmic effect of 9-phenanthrol could be demonstrated using the hypoxia–reoxygenation model described here. To our knowledge, this is the first report on the cardiac effects of a benzo[c]quinolizinium derivative.

The physiological effects of benzo[c]quinoliziniums have not been defined. A large family of these molecules was designed to modulate the cystic fibrosis transmembrane conductance regulator chloride channel (CFTR) (Becq *et al.*, 1999; Becq, 2006). The CFTR is expressed in the heart, albeit weakly, including in mouse ventricular cardiomyocytes (Lader *et al.*, 2000; Yamamoto-Mizuma *et al.*, 2004; Sellers *et al.*, 2010). However, since 9-phenanthrol does not have any effect on CFTR (Grand *et al.*, 2008), modulation of CFTR cannot explain the observed anti-arrhythmic effect of this compound.

In addition to CFTR, the ATP-sensitive K^+ channel (K_{ATP}) was shown to be inhibited by the benzo[c]quinolizinium MPB-91 in *Xenopus* oocytes (Prost *et al.*, 2003). K_{ATP} channel is activated under hypoxic conditions in cardiomyocytes, when $[ATP]_i$ is reduced (Benndorf *et al.*, 1991b) and causes cell hyperpolarization that protects against arrhythmias. Similar to MPB-91, 9-phenanthrol may inhibit the K_{ATP} channel. However, action potential prolongation through inhibition of K_{ATP} would have promoted (rather than inhibited) the phase 2 EADs observe in the present study, which is contrary to our results. Moreover, the lack of effect of 9-phenanthrol on the RMP indicates that the molecule does not modulate ionic channels that are opened during the diastolic potential, including K_{ATP} and the background inward rectifier I_{K1} channels. Hence, 9-phenanthrol is unlikely to act through K_{ATP} channel inhibition.

In our experiments, we observed that 9-phenanthrol, at a concentration of 10^{-5} mol·L^{-1}, had no effect on the global K^+ current, while at 10^{-4} mol·L^{-1}, 9-phenanthrol inhibited it by 43%. In this study, we have not determined precisely which component(s) of I_K was (were) implicated. Although a high concentration of 9-phenanthrol inhibits a part of the current, it is unlikely that this inhibition explains reduced frequency

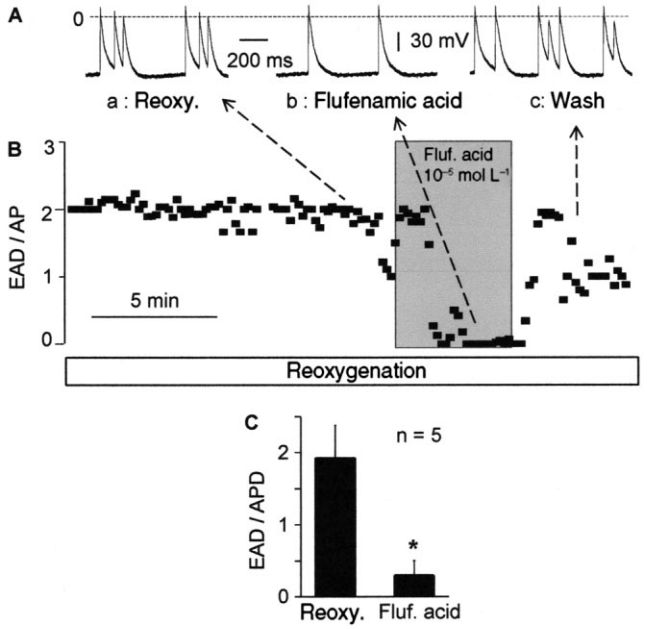

Figure 5

Anti-arrhythmic effect of flufenamic acid. (A) Action potentials recorded in a mouse ventricle superfused with standard re-oxygenation solution (a), followed by that containing flufenamic acid, 10^{-5} mol·L^{-1} (b), followed by wash with re-oxygenation solution without drug again (c). Bars represent the time interval (ms) and voltage (mV) as indicated. (B) Number of EAD/AP for 10 s periods during the above phases, as indicated by arrows. Phase (b) is highlighted in grey. Bar represents a 5 min interval. (C) EAD/AP (mean ± SEM) recorded during re-oxygenation with standard solution or with that containing flufenamic acid, 10^{-5} mol·L^{-1} are compared (n = 5).

of EADs since it would have had an opposite pro-arrhythmic effect.

A reduction in the frequency of EADs induced by 9-phenanthrol may be due to a direct inhibitory effect on L-type Ca^{2+} channels. Interestingly, we observed that 9-phenanthrol was able to inhibit $I_{Ca,L}$ at 10^{-4} mol·L^{-1} but had no effect at 10^{-5} mol·L^{-1}, a concentration at which frequency of EADs diminished by 76% in our model. Thus, even if, at a high concentration, $I_{Ca,L}$ is involved in the reduction of EADs induced by 9-phenanthrol, it is probably not the main target. This interpretation is also supported by the anti-arrhythmic effect of flufenamic acid that we observed at 10^{-5} mol·L^{-1}, a concentration shown to have no effect on $I_{Ca,L}$ in arteries (Shimamura *et al.*, 2002). It is known that EADs arising below –40 mV during late repolarization are most likely due to Ca^{2+}-dependent currents than to $I_{Ca,L}$ activation (Bers, 2001). Because the EADs recorded in our model occurred late in the repolarization phase(see Figures 1, 2, 4 and 5), the target of 9-phenanthrol is probably a Ca^{2+}-sensitive current.

The benzo[c]quinolizinium compounds, MPB-104 and 9-phenanthrol were shown to inhibit TRPM4 over-expressed in HEK-293 cells (Grand *et al.*, 2008). Moreover, TRPM4 is the only known channel to be affected by 9-phenanthrol. The TRPM4 current was inhibited by 30% with 10^{-5} mol·L^{-1} 9-phenanthrol and by 90% with 10^{-4} mol·L^{-1} 9-phenanthrol ($IC_{50} = 2 \times 10^{-5}$ mol·L^{-1}) (Grand *et al.*, 2008). This sensitivity of TRPM4 to 9-phenanthrol is in agreement with the effective concentrations for the anti-arrhythmic effect observed in terms of reduction of EADs occurrence in the present study; we observed a partial reduction in the frequency of EADs with 10^{-5} mol·L^{-1} 9-phenanthrol and abolition with 10^{-4} mol·L^{-1} 9-phenanthrol.

In view of the structural similarities among the TRP channels, 9-phenanthrol would be expected to modulate their activities. However, recent experimental data have shown 9-phenanthrol to be specific to TRPM4. It is ineffective on TRPM5, structurally and functionally the closest channel to TRPM4 in the family (Grand *et al.*, 2008). Also, in contrast to TRPM4, TRPM5 is not expressed in mouse heart (Pérez *et al.*, 2002; Murakami *et al.*, 2003). TRPC3 and TRPC6 are two channels with relatively ubiquitous expression including in cardiac tissue. TRPC3 was detected in mouse ventricular cardiomyocytes in which it participates in ischaemia–reperfusion-induced perturbations, increasing apoptosis (Shan *et al.*, 2008). TRPC6 is also expressed in mouse cardiomyocytes and, like TRPC3, is involved in hypertrophic signalling (Kinoshita *et al.*, 2010; Wu *et al.*, 2010). None of these channels, when expressed in HEK-293 cells, is affected by 9-phenanthrol (3.10^{-5} mol·L^{-1}) (Gonzales *et al.*, 2010b). 9-Phenanthrol was also shown to have no effect on a TRPM7-like current in mouse Cajal cells; TRPM7 is another member of the TRP family that is expressed in heart (Kim *et al.*, 2011). Similarly, 9-phenanthrol ($3x10^{-5}$ mol·L^{-1}) does not inhibit the vascular smooth muscle large conductance Ca^{2+}-activated K^+ current (BK_{Ca}), inward-rectifier K^+ current (IK_{IR}), voltage-dependent K^+ current (K_V) or voltage-dependent Ca^{2+} current (VDCa) (Gonzales *et al.*, 2010b).

Taken together, these data strongly suggest that 9-phenanthrol induces its anti-arrhythmic effect through inhibition of the TRPM4 channel. This hypothesis is also supported by the effect of flufenamic acid.

Anti-arrhythmic effect of flufenamic acid

Flufenamic acid is a non-steroidal anti-inflammatory drug shown to inhibit TRPM4 when overexpressed in HEK-293 cells (Ullrich *et al.*, 2005). Similar levels of inhibition were observed for endogenous TRPM4 in cardiomyocytes from human, rat and mouse (Guinamard *et al.*, 2004; 2006; Demion *et al.*, 2007). It is commonly used to study the physiological effects of TRPM4.

Flufenamic acid is also known to modulate the activity of a large variety of other ion channels including the Ca^{2+}-activated Cl^- channel (Greenwood and Large, 1995), the swelling-activated Cl^- channel (Jin *et al.*, 2003) and TRP channels such as TRPC3 and TRPC6 (Inoue *et al.*, 2001; Albert *et al.*, 2006), all of which are expressed in the heart. In addition, flufenamic acid was recently reported to activate a depolarizing cationic current different from TRPM4 in ventricular cardiomyocytes (Macianskiene *et al.*, 2010). Since flufenamic acid is a less specific inhibitor, its anti-arrhythmic effect observed here may involve other channels in addition to TRPM4. However, at least 10^{-4} mol·L^{-1} of flufenamic acid is required to effectively modulate other channels, including $I_{Ca,L}$ (Inoue *et al.*, 2001; Shimamura *et al.*, 2002). Whereas its concentration for half-maximal inhibition of TRPM4 was reported to be between 2.8 and 5.5 × 10^{-6} mol·L^{-1} (Ullrich

et al., 2005; Guinamard *et al.*, 2006), flufenamic acid at a concentration of 10^{-5} mol·L^{-1} reduced the frequency of EADs by 84% in the present study, and this concentration was reported to inhibit 70% of TRPM4 currents in cardiac cells (Guinamard *et al.*, 2006). Hence, it is likely that TRPM4 is the target affected by flufenamic acid in our experiments.

Regardless of the target of flufenamic acid, the inhibition of EADs is intriguing. So far, there have been few data reported on the effects of flufenamic acid on cardiac functions. A study on rat atrium reported that flufenamic acid exaggerated ischaemia-induced mechanical perturbations by enhancing the decline in the ATP store (Northover, 1989). To our knowledge, there is no available data regarding the effect of flufenamic acid on arrhythmias. Yet it is a matter of interest, since flufenamic acid doses used in clinical applications lead to serum concentrations of 1.4–4 × 10^{-5} mol·L^{-1}, similar to the concentration used in our study (Aly *et al.*, 2000).

TRPM4 in EAD induction

TRPM4 is a non-selective monovalent cation channel conducting Na^+ and K^+ ions with equal efficiency (Launay *et al.*, 2002). Hence, it is suspected to maintain the resting membrane potential at 0 mV when activated, if one considers that the internal and external concentrations for total monovalent cations are equivalent. In the time course of a cardiac action potential, two parameters would favour TRPM4 activation: firstly the voltage reached during the overshoot and the plateau phase, because TRPM4 is a non-inactivating voltage-dependent channel with increased activity at depolarized voltages (Launay *et al.*, 2002; Nilius *et al.*, 2003); secondly, the cytoplasmic calcium transient because TRPM4 is an intracellular-Ca^{2+}-activated channel (Launay *et al.*, 2002). TRPM4 would thus slow down the repolarization. Slowing of the repolarization process is favourable for reactivation of the Ca^{2+} current and thus appearance of EADs (Carmeliet, 1999). Interestingly, we have previously reported an overexpression of TRPM4 in cardiac hypertrophy (Guinamard *et al.*, 2006), a pathology known to be associated with an increased occurrence of EADs in the rabbit (Yan *et al.*, 2001). It is noteworthy that 9-phenanthrol did not affected RMP in our study, suggesting that the TRPM4 channel was already closed because of the negative voltage and low calcium level at the diastolic potential. TRPM4 would thus participate in triggered arrhythmias but may not induce spontaneous activity in the ventricle.

In conclusion, our data indicate that 9-phenanthrol, a benzo[c]quinolizinium derivative, can reduce cardiac arrhythmia, most likely due to its inhibition of TRPM4 channel. Thus, while classical therapeutic approaches target specific K^+, Na^+ or Ca^{2+} channels, non-selective cation channel inhibitors may be effective pharmacological agents in the treatment of cardiac arrhythmias.

Acknowledgements

The authors thank Hervé Tombette, Sandrine Lemoine and Zakkia Kaddache for technical help and Dr Anuradha Alahari for editing the manuscript.

Funding

CS received a PhD fellowship from the French Ministry of Education and Research. RG, LS and RR are employed by the French Ministry of Education and Research.

Conflicts of interest

The authors state no conflict of interest.

References

Albert AP, Pucovsky V, Prestwich SA, Large WA (2006). TRPC3 properties of a native constitutively active Ca2+-permeable cation channel in rabbit ear artery myocytes. J Physiol 571: 361–369.

Alexander SPH, Mathie A, Peters JA (2011). Guide to Receptors and Channels (GRAC), 5th edition. Br J Pharmacol 164 (Suppl. 1): S1–S324.

Aly FA, Al-Tamimi SA, Alwarthan AA (2000). Determination of flufenamic acid and mefenamic acid in pharmaceutical preparations and biological fluids using flow injection analysis with tris(2,2′-bipyridyl)ruthenium(II) chemiluminescence detection. Anal Chim Acta 416: 87–96.

Anumonwo JM, Tallini YN, Vetter FJ, Jalife J (2001). Action potential characteristics and arrhythmogenic properties of the cardiac conduction system of the murine heart. Circ Res 89: 329–335.

Becq F (2006). On the discovery and development of CFTR chloride channel activators. Curr Pharm Des 12: 471–484.

Becq F, Mettey Y, Gray MA, Galietta LJ, Dormer RL, Merten M *et al.* (1999). Development of substituted Benzo[c]quinolizinium compounds as novel activators of the cystic fibrosis chloride channel. J Biol Chem 274: 27415–27425.

Benndorf K, Friedrich M, Hirche H (1991a). Reoxygenation-induced arrhythmogenic transient inward currents in isolated cells of the guinea-pig heart. Pflugers Arch 418: 248–260.

Benndorf K, Friedrich M, Hirche H (1991b). Anoxia opens ATP regulated K channels in isolated heart cells of the guinea pig. Pflugers Arch 419: 108–110.

Bers DM (2001). Cardiac action potential and ion channels. In: Kluwer Academic Publishers (ed.). Excitation-Contraction Coupling and Cardiac Contractile Force, 2nd edn. Kluwer Academic Publishers: Dordrecht, pp. 63–100.

Brette F, Leroy J, Le Guennec JY, Sallé L (2006). Ca^{2+} currents in cardiac myocytes: old story, new insights [Review]. Prog Biophys Mol Biol 91: 1–82.

Carmeliet E (1999). Cardiac ionic currents and acute ischemia: from channels to arrhythmias. Physiol Rev 79: 917–1017.

Chijiwa T, Mishima A, Hagiwara M, Sano M, Hayashi K, Inoue T *et al.* (1990). Inhibition of forskolin-induced neurite outgrowth and protein phosphorylation by a newly synthesized selective inhibitor of cyclic AMP-dependent protein kinase, *N*-[2-(*p*-bromocinnamylamino)ethyl]-5-isoquinolinesulfonamide (H-89), of PC12D pheochromocytoma cells. J Biol Chem 265: 5267–5272.

Demion M, Bois P, Launay P, Guinamard R (2007). TRPM4, a Ca2+-activated nonselective cation channel in mouse sino-atrial node cells. Cardiovasc Res 73: 531–538.

Gonzales AL, Amberg GC, Earley S (2010a). Ca2+ release from the sarcoplasmic reticulum is required for sustained TRPM4 activity in cerebral artery smooth muscle cells. Am J Physiol Cell Physiol 299: C279–C288.

Gonzales AL, Garcia ZI, Amberg GC, Earley S (2010b). Pharmacological Inhibition of TRPM4 Hyperpolarizes Vascular Smooth Muscle. Am J Physiol Cell Physiol 299: C1195–C1202.

Grand T, Demion M, Norez C, Mettey Y, Launay P, Becq F *et al.* (2008). 9-phenanthrol inhibits human TRPM4 but not TRPM5 cationic channels. Br J Pharmacol 153: 1697–1705.

Greenwood IA, Large WA (1995). Comparison of the effects of fenamates on Ca-activated chloride and potassium currents in rabbit portal vein smooth muscle cells. Br J Pharmacol 116: 2939–2948.

Guinamard R, Chatelier A, Demion M, Potreau D, Patri S, Rahmati M *et al.* (2004). Functional characterization of a Ca(2+)-activated non-selective cation channel in human atrial cardiomyocytes. J Physiol 558: 75–83.

Guinamard R, Demion M, Magaud C, Potreau D, Bois P (2006). Functionnal expression of the TRPM4 cationic current in ventricular cardiomyocytes from spontaneously hypertensive rats. Hypertension 48: 587–594.

Guinamard R, Demion M, Launay P (2010). Physiological roles of the TRPM4 channel extracted from background currents. Physiology 25: 155–164.

Inoue R, Okada T, Onoue H, Hara Y, Shimizu S, Naitoh S *et al.* (2001). The transient receptor potential protein homologue TRP6 is the essential component of vascular alpha(1)-adrenoceptor-activated Ca(2+)-permeable cation channel. Circ Res 88: 325–332.

Jin NG, Kim JK, Yang DK, Cho SJ, Kim JM, Koh EJ *et al.* (2003). Fundamental role of ClC-3 in volume-sensitive Cl- channel function and cell volume regulation in AGS cells. Am J Physiol Gastrointest Liver Physiol 285: G938–G948.

Kihara Y, Grossman W, Morgan JP (1989). Direct measurement of changes in intracellular calcium transients during hypoxia, ischemia, and reperfusion of the intact mammalian heart. Circ Res 65: 1029–1044.

Kim BJ, Nam JH, Kim SJ (2011). Effects of transient receptor potential channel blockers on pacemaker activity in interstitial cells of Cajal from mouse small intestine. Mol Cells 32: 153–160.

Kinoshita H, Kuwahara K, Nishida M, Jian Z, Rong X, Kiyonaka S *et al.* (2010). Inhibition of TRPC6 channel activity contributes to the antihypertrophic effects of natriuretic peptides-guanylyl cyclase-A signaling in the heart. Circ Res 106: 1849–1860.

Kruse M, Schulze-Bahr E, Corfield V, Beckmann A, Stallmeyer B, Kurtbay G *et al.* (2009). Impaired endocytosis of the ion channel TRPM4 is associated with human progressive familial heart block type I. J Clin Invest 119: 2737–2744.

Lader AS, Wang Y, Jackson GR Jr, Borkan SC, Cantiello HF (2000). cAMP-activated anion conductance is associated with expression of CFTR in neonatal mouse cardiac myocytes. Am J Physiol Cell Physiol 278: C436–C450.

Launay P, Fleig A, Perraud AL, Scharenberg AM, Penner R, Kinet JP (2002). TRPM4 is a Ca2+-activated nonselective cation channel mediating cell membrane depolarization. Cell 109: 397–407.

Liu H, El Zein L, Kruse M, Guinamard R, Beckmann A, Bozio A *et al.* (2010). Gain-of-function mutations in TRPM4 cause autosomal dominant isolated cardiac conduction disease. Circ Cardiovasc Genet 3: 374–385.

Lochner A, Moolman JA (2006). The many faces of H89: a review. Cardiovasc Drug Rev 24: 261–274.

Macianskiene R, Gwanyanya A, Sipido KR, Vereecke J, Mubagwa K (2010). Induction of a novel cation current in cardiac ventricular myocytes by flufenamic acid and related drugs. Br J Pharmacol 161: 416–429.

Mrejeru A, Wei A, Ramirez JM (2011). CAN currents are involved in generation of tonic and bursting activity in dopamine neurons of the substantia nigra pars compacta. J Physiol 589: 2497–2514.

Murakami M, Xu F, Miyoshi I, Sato E, Ono K, Iijima T (2003). Identification and characterization of the murine TRPM4 channel. Biochem Biophys Res Commun 307: 522–528.

Nerbonne JM, Kass RS (2005). Molecular physiology of cardiac repolarization. Physiol Rev 85: 1205–1253.

Nilius B, Prenen J, Droogmans G, Voets T, Vennekens R, Freichel M *et al.* (2003). Voltage dependence of the Ca2+-activated cation channel TRPM4. J Biol Chem 278: 30813–30820.

Northover BJ (1989). The involvement of lactate and calcium as mediators of the electrical and mechanical response of the myocardium to conditions of simulated ischaemia. Br J Pharmacol 97: 809–818.

Pérez CA, Huang L, Rong M, Kozak JA, Preuss AK, Zhang H *et al.* (2002). A transient receptor potential channel expressed in taste receptor cells. Nat Neurosci 5: 1169–1176.

Priori SG, Mantica M, Napolitano C, Schwartz PJ (1990). Early afterdepolarizations induced in vivo by reperfusion of ischemic myocardium. A possible mechanism for reperfusion arrhythmias. Circulation 81: 1911–1920.

Prost A, Dérand R, Gros L, Becq F, Vivaudou M (2003). Inhibition of ATP-sensitive K+ channels by substituted benzo[c]quinolizinium CFTR activators. Biochem Pharmacol 66: 425–430.

Robinet A, Hoizey G, Millart H (2005). PI 3-kinase, protein kinase C, and protein kinase A are involved in the trigger phase of b1-adrenergic preconditionong. Cardiovasc Res 66: 530–542.

Sallé L, Kharche S, Zhang H, Brette F (2008). Mechanisms underlying adaptation of action potential duration by pacing rate in rat myocytes. Prog Biophys Mol Biol 96: 305–320.

Sellers ZM, De Arcangelis V, Xiang Y, Best PM (2010). Cardiomyocytes with disrupted CFTR function require CaMKII and Ca(2+)-activated Cl(-) channel activity to maintain contraction rate. J Physiol 588: 2417–2429.

Shan D, Marchase RB, Chatham JC (2008). Overexpression of TRPC3 increases apoptosis but not necrosis in response to ischemia-reperfusion in adult mouse cardiomyocytes. Am J Physiol Cell Physiol 294: C833–C841.

Shen H, Liu TF (1993). Generation of early afterdepolarization in mouse ventricular fibers at long cycle length. Methods Find Exp Clin Pharmacol 15: 15–21.

Shimamura K, Zhou M, Ito Y, Kimura S, Zou LB, Sekiguchi F *et al.* (2002). Effects of flufenamic acid on smooth muscle of the carotid artery isolated from spontaneously hypertensive rats. J Smooth Muscle Res 38: 39–50.

Siegmund B, Zude R, Piper HM (1992). Recovery of anoxic-reoxygenated cardiomyocytes from severe Ca2+ overload. Am J Physiol 263: H1262–H1269.

Stables CL, Curtis MJ (2009). Development and characterization of a mouse in vitro model of ischaemia-induced ventricular fibrillation. Cardiovasc Res 83: 397–404.

Sugimoto S, Puddu PE, Monti F, Dawodu AA, del Monte F, Schiariti M *et al*. (1995). Activation of ATP-dependent K+ channels enhances myocardial protection due to cold high potassium cardioplegia: a force-frequency relationship study. J Mol Cell Cardiol 27: 1867–1881.

Ullrich ND, Voets T, Prenen J, Vennekens R, Talavera K, Droogmans G *et al*. (2005). Comparison of functional properties of the Ca2+-activated cation channels TRPM4 and TRPM5 from mice. Cell Calcium 37: 267–278.

Wang BH, Ternai B, Polya GM (1994). Specific inhibition of cyclic AMP-dependent protein kinase by the antimalarial halofantrine and by related phenanthrenes. Biol Chem Hoppe Seyler 375: 527–535.

Wu X, Eder P, Chang B, Molkentin JD (2010). TRPC channels are necessary mediators of pathologic cardiac hypertrophy. Proc Natl Acad Sci U S A 107: 7000–7005.

Yamamoto-Mizuma S, Wang GX, Hume JR (2004). P2Y purinergic receptor regulation of CFTR chloride channels in mouse cardiac myocytes. J Physiol 556: 727–737.

Yan GX, Rials SJ, Wu Y, Liu T, Xu X, Marinchak RA *et al*. (2001). Ventricular hypertrophy amplifies transmural repolarization dispersion and induces early afterdepolarization. Am J Physiol Heart Circ Physiol 28: H1968–H1975.

Zhou YY, Liu TF (1997). The ionic mechanisms of early after depolarization in mouse ventricular myocytes: the role of IK1. Methods Find Exp Clin Pharmacol 19: 443–453.